© 2016. Published by The Company of Biologists Ltd | Development (2016) 143, 211-218 doi:10.1242/dev.128793

Genetic analysis of Runx2 function during intramembranous ossification

Takeshi Takarada*, Ryota Nakazato, Azusa Tsuchikane, Koichi Fujikawa, Takashi Iezaki, Yukio Yoneda and Eiichi Hinoi*

ABSTRACT

Runt-related transcription factor 2 (Runx2) is an essential transcriptional regulator of osteoblast differentiation and its haploinsufficiency leads to cleidocranial dysplasia because of a defect in osteoblast differentiation during bone formation through intramembranous ossification. The cellular origin and essential period for Runx2 function during osteoblast differentiation in intramembranous ossification remain poorly understood. Paired related homeobox 1 (Prx1) is expressed in craniofacial mesenchyme, and Runx2 deficiency in cells of the Prx1 lineage (in mice referred to here as *Runx2*$_{prx1}^{-/-}$) resulted in defective intramembranous ossification. Runx2 was heterogeneously expressed in Prx1-GFP^{+} cells located at the intrasutural mesenchyme in the calvaria of transgenic mice expressing GFP under the control of the *Prx1* promoter. Double-positive cells for Prx1-GFP and stem cell antigen-1 (Sca1) (Prx1^{+}Sca1^{+} cells) in the calvaria expressed *Runx2* at lower levels and were more homogeneous and primitive than Prx1^{+}Sca1^{-} cells. Osterix (Osx) is another transcriptional determinant of osteoblast lineages expressed by osteoblast precursors; Osx is highly expressed by Prx1^{-}Runx2^{+} cells at the osteogenic front and on the surface of mineralized bone in the calvaria. Runx2 deficiency in cells of the Osx lineage (in mice referred to here as *Runx2*$_{osx}^{-/-}$) resulted in severe defects in intramembranous ossification. These findings indicate that the essential period of Runx2 function in intramembranous ossification begins at the Prx1^{+}Sca1^{+} mesenchymal stem cell stage and ends at the Osx^{+}Prx1^{-}Sca1^{-} osteoblast precursor stage.

KEY WORDS: Nestin, Osteoblast, Osterix, Prx1, Runx2, Mouse

INTRODUCTION

Bone is generated by two distinct skeletal ossification processes during embryonic and postnatal skeletogenesis. Bones in the calvaria, such as the frontal and parietal bones, ossify through intramembranous ossification, whereas other bones, such as the long bones and vertebrae ossify through endochondral ossification. In the endochondral ossification process, a cartilaginous template is first formed by condensation of mesenchymal stem cells (MSCs), which then differentiate into chondrocytes. Chondrocytes successively proliferate and then undergo hypertrophy and apoptosis through a well-organized mechanism. Upon apoptosis of chondrocytes, capillaries, osteoclasts, bone marrow cells, and osteoblasts begin to invade the cartilage matrix to produce new bones (Kronenberg, 2003). By contrast, in intramembranous ossification, MSCs undergo differentiation into osteoprogenitor cells, and subsequently proliferate and differentiate into osteoblasts that express type I collagen, osteopontin (Opn; Spp1 – Mouse Genome Informatics) and osteocalcin (also known as bone γ carboxyglutamate protein), and synthesize bone matrix (Hall and Miyake, 1992). Osteoblast differentiation occurs at the osteogenic fronts, where progenitor cells are recruited from the surrounding mesenchyme. The calvarial bones grow as sheets between the brain and epidermis, and a suture is responsible for the maintenance of separation between calvarial bones.

Runt-related transcription factor 2 (Runx2) is a cell-specific member of the Runt transcription factor family, which is considered the master gene of osteoblast differentiation (Ducy et al., 1997; Komori et al., 1997). *RUNX2* haploinsufficiency causes cleidocranial dysplasia, an autosomal-dominant human bone disease characterized by defective intramembranous ossification with hypoplastic clavicles, patent fontanelles, and sutures (Mundlos et al., 1997; Otto et al., 1997). We recently showed that osteoblast-specific deletion of *Runx2* using *α1(I)-collagen-Cre* (referred to here as *Runx2*$_{col(I)}^{-/-}$) mice resulted in no overt abnormalities (Takarada et al., 2013). These results indicated that Runx2 is dispensable in α1(I)-collagen-expressing osteoblasts. Hence, the stage of osteoblast differentiation at which Runx2 is necessary remains to be determined. Less is known about the overall differentiation process and the contribution of Runx2 in intramembranous ossification than during endochondral bone formation despite the simpler process of osteoblast differentiation in intramembranous ossification.

Paired related homeobox 1 (Prx1; Prrx1 – Mouse Genome Informatics) is expressed in MSCs in the limb buds and craniofacial mesenchyme (Cserjesi et al., 1992), and the intermediate filament protein nestin, which was first reported as a marker of neuroectoderm progenitors (Lendahl et al., 1990), is also a marker of MSCs (Méndez-Ferrer et al., 2010). Here, we showed that Runx2 is essential for intramembranous ossification through its expression in cells of the Prx1 lineage but not in cells of the nestin lineage. In addition, we also examined the localization of Prx1-GFP- and nestin-GFP-expressing cell populations in calvaria, and showed that Runx2 is heterogeneously expressed in Prx1-GFP^{+} cells, but not nestin-GFP^{+} cells. Functional *in vitro* analysis indicated that Prx1-GFP^{+}Sca1^{+} cells expressed lower levels of Runx2 and were more primitive in terms of multipotency and self-renewal than were Prx1-GFP^{+}Sca1^{-} cells. Moreover, we showed that Runx2 is also required for intramembranous ossification through its expression in cells of the osterix (Osx; Sp7 – Mouse Genome Informatics) lineage. Our results demonstrate that the essential period of Runx2 function in intramembranous ossification begins at the Prx1^{+}Sca1^{+} mesenchymal stem cell stage and ends at the Osx^{+}Prx1^{-}Sca1^{-} osteoblast precursor stage.

Laboratory of Molecular Pharmacology, Division of Pharmaceutical Sciences, Kanazawa University Graduate School, Kanazawa, Ishikawa 920-1192, Japan.

*Authors for correspondence (takarada@p.kanazawa-u.ac.jp; hinoi@p.kanazawa-u.ac.jp)

Received 22 July 2015; Accepted 28 November 2015

Development (2016) 143, 211-218 doi:10.1242/dev.128793

RESULTS AND DISCUSSION

Runx2 is required for intramembranous ossification in cells of the Prx1 lineage, but not cells of the nestin lineage

To identify the cell type in which Runx2 must be activated for intramembranous ossification, we employed two types of Cre drivers, *Prx1-Cre* mice (Logan et al., 2002) and *Nestin-Cre* mice, which express Cre recombinase under the control of the 2.4-kb *Prx1* promoter or the 5.8-kb promoter and 1.8-kb second intron of the *Nes* gene (Zimmerman et al., 1994), respectively.

Although *Prx1-Cre;Runx2*$^{flox/flox}$ (*Runx2*$_{prx1}$$^{-/-}$) embryos were alive at embryonic day (E) 18.5, they died at birth because of breathing difficulties. The perinatal lethality of *Runx2*$_{prx1}$$^{-/-}$ mice was almost similar to that observed in *Runx2*$^{-/-}$ mice (Takarada et al., 2013). By contrast, *Runx2*$_{nestin}$$^{-/-}$ mice were born at the frequency predicted by the Mendelian principles of inheritance (data not shown). Alizarin Red and Alcian Blue staining of skeletal preparations of E18.5 embryos of *Runx2*$_{prx1}$$^{-/-}$ and *Runx2*$_{nestin}$$^{-/-}$ mice was performed (Fig. 1A). *Runx2*$_{nestin}$$^{-/-}$ embryos had no marked abnormalities in skeletal development, compared with wild-type (WT) embryos. By contrast, *Runx2*$_{prx1}$$^{-/-}$ embryos showed severe mineralization defects in the calvaria, scapula, humerus, radius, ulna, femur, tibia, fibula and sternum. Moreover, the clavicles of these *Runx2*$_{prx1}$$^{-/-}$ embryos were extremely hypoplastic (Fig. 1B, arrow). It is important to note that, in contrast to the skeletal phenotypes of *Runx2*$_{col(II)}$$^{-/-}$ mice (Takarada et al., 2013), *Runx2*$_{prx1}$$^{-/-}$ embryos lacked bones that are formed through either endochondral or intramembranous ossification (Fig. 1B).

Immunohistochemical analyses revealed that expression of the osteogenic markers Osx and Opn, in addition to Runx2, were absent in the parietal bone of *Runx2*$_{prx1}$$^{-/-}$ mice (Fig. S1A). In addition, adipogenic (fatty acid binding protein 4) and chondrogenic (type II collagen) markers were not detected in parietal bone of either WT or *Runx2*$_{prx1}$$^{-/-}$ mice (Fig. S1A). Moreover, *in vitro* studies revealed that *Runx2*$_{prx1}$$^{-/-}$ mouse-derived calvarial cells, in which the expression of *Runx2*, but not *Prx1*, was decreased (Fig. S1B), had less bone-forming potential than those of WT mice (Fig. S1C).

To reveal the phenotypic differences in Runx2 deficiency between cells of the Prx1 lineage and cells of the nestin lineage, we generated *Prx1-Cre;Rosa26-tdTomato* mice and *Nestin-Cre;Rosa26-tdTomato* mice, in which cells expressing Prx1 or nestin and their descendants become Tomato^{+}, to track cell fates (Fig. 1C,E). In *Prx1-Cre;Rosa26-tdTomato* mice, Tomato^{+} cells (cells of the Prx1 lineage) were widely distributed in the parietal bone, including intrasutural mesenchyme, osteogenic front, and bony plate surface, and overlapped with Runx2 at the osteogenic front and the bony plate surface in addition to the intrasutural mesenchyme, and with Osx and Opn at the bony plate surface (Fig. 1D; Fig. S2A,B). Almost all Runx2-, Osx- and Opn-positive cells were Tomato positive (cells of the Prx1 lineage) (Fig. S3A), indicating that almost all osteoblasts were derived from the Prx1 lineage, at least in the parietal bone of newborn mice.

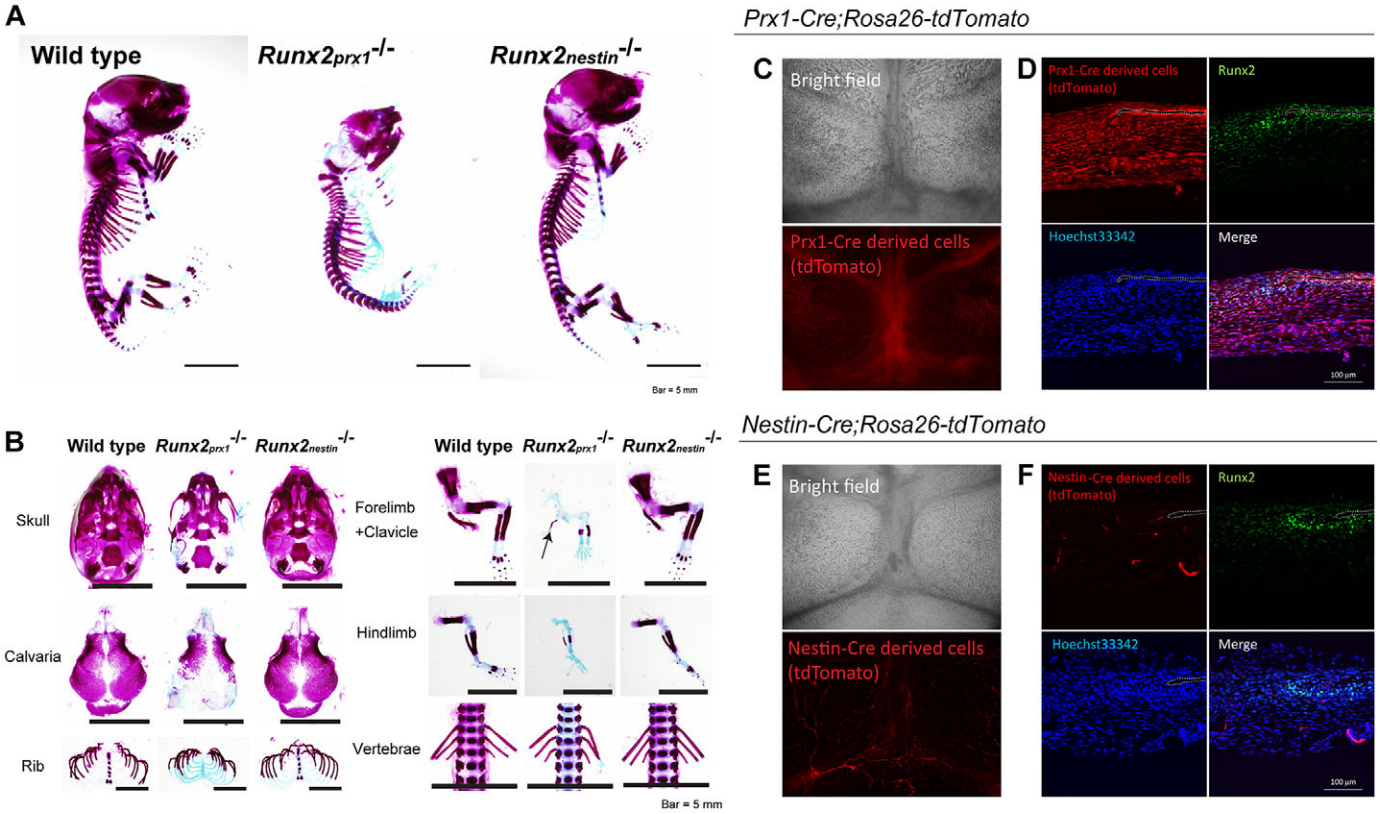

Fig. 1. Runx2 is required for intramembranous ossification through its expression in cells of the Prx1 lineage. (A) The skeleton of wild-type (WT), *Runx2*$_{prx1}$$^{-/-}$ and *Runx2*$_{nestin}$$^{-/-}$ mice at E18.5. Embryos were double stained with Alizarin Red and Alcian Blue. (B) Parts of the skeleton from WT, *Runx2*$_{prx1}$$^{-/-}$ and *Runx2*$_{nestin}$$^{-/-}$ mice at E18.5. The clavicle was hypoplastic in *Runx2*$_{prx1}$$^{-/-}$ mice (arrow). (C) tdTomato fluorescence in the calvaria of *Prx1-Cre;Rosa26-tdTomato* mice at P1. (D) Confocal image of the sagittal suture of *Prx1-Cre;Rosa26-tdTomato* mice at P1. Sections were stained with an anti-Runx2 antibody (green). (E) tdTomato fluorescence in the calvaria of *Nestin-Cre;Rosa26-tdTomato* mice at P1. (F) Confocal image of the sagittal suture of *Nestin-Cre;Rosa26-tdTomato* mice at P1. The sections were stained with an anti-Runx2 antibody (green). Scale bars: 5 mm (A,B); 100 µm (D,F).

Development (2016) 143, 211-218 doi:10.1242/dev.128793

In contrast to cells of the Prx1 lineage, in *Nestin-Cre;Rosa26-tdTomato* mice, Tomato$^+$ cells (cells of the nestin lineage) were found in the parietal bone, and were completely separated from Runx2-expressing cells at postnatal day (P) 1 (Fig. 1F), P10 and 12 weeks old (Fig. S4A). Moreover, Runx2 mRNA expression was comparable in WT and *Runx2*$_{nestin}^{-/-}$ mouse-derived calvarial cells (Fig. S4B), and the intensity of immunostaining for Runx2 in parietal bone of adult mice was also comparable in WT and *Runx2*$_{nestin}^{-/-}$ mice (Fig. S4C). Moreover, Tomato$^+$ cells (cells of the nestin lineage) did not express Osx or Opn in the parietal bone at P1 (Fig. S2C,D) and P10 (Fig. S4A), suggesting that the *Nestin-Cre* driver used in this study does not target osteoblasts in calvaria, which supports the lack of a skeletal phenotype at E18.5 and the lack of abnormalities in calvaria of 6-month-old *Runx2*$_{nestin}^{-/-}$ mice (Fig. 1A,B; Fig. S4D).

In contrast to parietal bone, in *Prx1-Cre;Rosa26-tdTomato* mice, Tomato$^+$ cells (cells of the Prx1 lineage) were scattered in the frontal bone (Fig. S5A,B), but some overlapped with Osx and Opn at the surface of the bony plate (Fig. S5C). The fact that the recombination efficiency of the *Prx1-Cre* driver was reduced in frontal bone, compared with that in parietal bone, might lead to the phenotypic differences in mineralization between parietal and frontal bone in *Runx2*$_{prx1}^{-/-}$ mice (Fig. 1B). Moreover, this could possibly explain why *Runx2*$_{prx1}^{-/-}$ mice had a greater extent of mineralization in frontal bone, compared with that of *Runx2*$^{-/-}$ mice. As it has been reported that the entire frontal bone is derived from the cranial neural crest, whereas other skull bones principally originate from the paraxial mesoderm (Chai and Maxson, 2006), *Wnt1-Cre*, which is a known reporter of neural crest origin (Jiang et al., 2002; Yoshida et al., 2008), could be used to determine whether Runx2 affects frontal bone formation. Taken together, these results revealed that almost all osteoblasts are from the Prx1 lineage, at least in parietal bone of newborn mice, and Runx2 is essential for intramembranous ossification through its expression in cells of the Prx1 lineage, but not in cells of the nestin lineage.

Runx2 is expressed in Prx1-GFP$^+$ cells, but not nestin-GFP$^+$ cells, in the calvaria

Next, we assessed Runx2 expression in the calvaria of transgenic mice expressing green fluorescent protein (GFP) under control of the 2.4-kb *Prx1* promoter (Prx1-GFP$^+$) (Kawanami et al., 2009) or the 5.8-kb promoter and 1.8-kb second intron of the *Nes* gene (nestin-GFP$^+$) (Mignone et al., 2004; Ono et al., 2014). Whole-mount and histological analyses revealed the presence of Prx1-GFP$^+$ cells in the calvarial suture region (Fig. 2A). Immunostaining showed that Runx2 was highly expressed in Prx1-GFP$^-$ cells at the osteogenic front and the bony plate surface (mineralized bone), in addition to Prx1-GFP$^+$ cells at the intrasutural mesenchyme in parietal bone (Fig. 2B; Fig. S6A). As shown in Fig. S3B, 91.4% of Prx1-GFP$^+$ cells were positive for Runx2. Among Prx1-GFP$^+$ cells in the intrasutural mesenchyme, at least two cell types appear to be present: Prx1-GFP$^+$ cells expressing Runx2 at higher levels (Runx2^{hi}Prx1$^+$ cells; Fig. S7A, arrows) or at lower levels (Runx2^{low}Prx1$^+$ cells; Fig. S7A, arrowheads). Moreover, heterogeneous Runx2 expression in Prx1-GFP$^+$ cells was defined when a reference nuclear marker, Hoechst33342, was used as the standard (Fig. S7B).

To perform a direct comparison of Prx1-GFP$^+$ cells and *Prx1-Cre*-targeted cells in the parietal bone of newborn mice, we generated triple-transgenic mice carrying *Prx1-GFP*, *Prx1-Cre* and a *Rosa26-tdTomato* reporter (*Prx1-GFP;Prx1-Cre;Rosa26-tdTomato* mice) (Fig. S8). These mice revealed that all Prx1-GFP$^+$ cells overlapped with *Prx1-Cre*-targeted cells. Moreover, together with the results shown in Fig. S2A,B and Fig. S3A, almost all Osx$^+$ and Opn$^+$ osteoblasts appear to be Tomato$^+$Prx1-GFP$^-$ cells. In addition, almost all Prx1-GFP$^+$ cells expressed Runx2 (Fig. 2B; Fig. S3B) and all Runx2-expressing cells were *Prx1-Cre*-targeted cells (Fig. 1D; Fig. S3A). Although further experiments should be performed to reveal the cell types of Tomato$^+$Prx1-GFP$^-$Osx$^-$Opn$^-$ cells, these results indicate that *Prx1-Cre* could target and encompass all populations with the *Prx1-GFP* allele, and that Prx1$^+$ cells could give rise to the calvarial osteoblasts expressing Runx2, Osx and Opn *in vivo*.

In sharp contrast to Prx1-GFP$^+$ cells, nestin-GFP$^+$ cells did not express Runx2 protein in the parietal bone of the calvaria (Fig. 2C; Fig. S3B; Fig. S6B) along with markedly lower *Runx2* mRNA expression in GFP cells sorted from calvaria of *Nestin-GFP* mice compared with that of WT mice-derived calvarial cells (Fig. S9A). Together with the normal skeletal phenotype of *Runx2*$_{nestin}^{-/-}$ mice, the present studies imply that nestin$^+$ cells might not be required for generation of bone-forming osteoblasts in the calvaria. However, a recent paper by Ono et al. clearly revealed that vasculature-associated cells expressing nestin-GFP encompass early osteoblasts in endochondral ossification (Ono et al., 2014). To delineate the difference between cell types (nestin-GFP$^+$ cells and *Nestin-Cre*-targeted cells) that are differentially targeted in the parietal bone of newborn mice, therefore, we generated triple-transgenic mice carrying *Nestin-GFP*, *Nestin-Cre* and a *Rosa26-tdTomato* reporter (*Nestin-GFP;Nestin-Cre;Rosa26-tdTomato* mice) (Fig. S9B). These mice revealed that almost all cells targeted by *Nestin-Cre* were positive for nestin-GFP, whereas nestin-GFP$^+$ cells partially overlapped with *Nestin-Cre*-targeted cells (50.4±10.2%), suggesting that *Nestin-Cre* preferentially targets a subpopulation of nestin-GFP$^+$ cells in the parietal bone of the calvaria (Fig. S9C). These results might indicate problems with one of the *Nes* promoters, at least in calvarial cells. However, because immunohistochemical analyses revealed that Runx2 was not expressed in both nestin-GFP$^+$ cells and *Nestin-Cre*-targeted cells in the parietal bone of newborn mice, nestin$^+$ cells might not be required for generating bone-forming osteoblasts in the calvaria under the experimental conditions (including the mouse line) used in this study.

Prx1$^+$Sca1$^+$ cells expressed lower levels of Runx2 and can differentiate into both osteoblasts and adipocytes

Because Runx2 appears to be heterogeneously expressed in Prx1-GFP$^+$ cells, as shown in Fig. 2B and Fig. S7, and *Prx1-Cre* can target all populations of cells with the *Prx1-GFP* allele (Fig. S8), we next classified the populations of Prx1-GFP$^+$ cells according to the expression of various MSC surface markers. Cells were isolated from the parietal and frontal bone, including coronal and sagittal suture, and then subjected to flow cytometric analysis. To investigate the size of the fraction of cells coming from the differentiated calvaria and suture region, we used *α1(I)-collagen-Cre;Rosa26-tdTomato* mice, in which cells expressing α1(I)-collagen and their descendants become Tomato$^+$, and *Prx1-GFP* mice, in which GFP$^+$ cells are localized at the intrasutural mesenchyme but not at the osteogenic front and the bony plate surface in the calvaria. Among the total cells isolated from *α1(I)-collagen-Cre;Rosa26-tdTomato* mice, 10.1% were Tomato$^+$ cells (Fig. S10A), whereas among the total cells isolated from *Prx1-GFP* mice, 11.5% were GFP$^+$ cells (Fig. S10B). These results indicate that ∼10% of isolated total cells were from differentiated calvaria and the suture region in our experimental conditions.

Development (2016) 143, 211-218 doi:10.1242/dev.128793

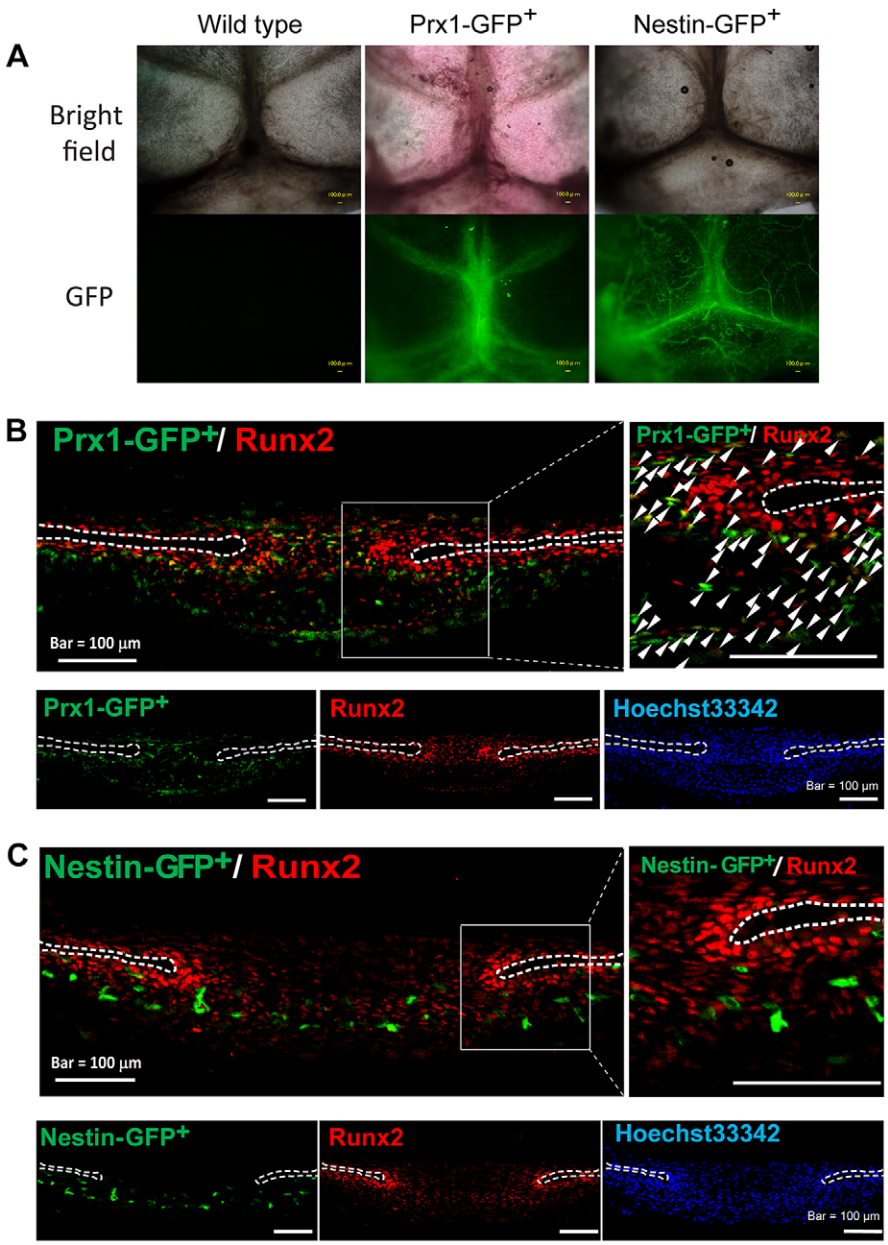

Fig. 2. Heterogeneous expression of Runx2 in Prx1-GFP$^+$ cells. (A) GFP fluorescence in the calvaria of wild-type (WT), *Prx1-GFP* and *Nestin-GFP* mice at P1. Scale bars: 100 µm. (B) Confocal image of the sagittal suture of *Prx1-GFP* mice at P1. Sections were stained with an anti-Runx2 antibody (red). The right-hand panels are magnified confocal images of the area defined by the square. Arrowheads indicate Runx2 and Prx1-GFP double-positive cells. (C) Confocal image of the sagittal suture of *Nestin-GFP* mice at P1. Dashed line indicates the border of mineralized bone.

In Prx1-GFP$^+$ cells of the calvaria, CD29, CD49e and CD51 (Itgb1, Itga5 and Itgav, respectively – Mouse Genome Informatics) were highly expressed, whereas platelet-derived growth factor receptor α (PDGFRα) and CD105, CD90, CD61 and stem cell antigen-1 (Sca1) (Eng, Thy1, Itgb3 and Ly6a, respectively – Mouse Genome Informatics) were significantly expressed to a lesser extent. As expected, the perivascular marker PDGFRβ, the endothelial marker CD31 (Pecam1– Mouse Genome Informatics), and the hematopoietic markers CD45 and Ter119 (Ptprc and Ly76, respectively – Mouse Genome Informatics) were not expressed by Prx1-GFP$^+$ cells (Fig. 3A; Fig. S11A). Recent studies revealed that mouse MSCs in the bone marrow are highly concentrated in populations of cells double-positive PDGFRα and Sca1 (PαS) (Morikawa et al., 2009). Flow cytometric analysis revealed that PαS cells comprised a small subset of Prx1-GFP$^+$ cells in the calvaria, and 8.4% were Prx1-GFP$^+$ cells among PαS cells (Fig. 3A; Fig. S11A).

Because Sca1 alone (10.1±5.3%) was present in a similar percentage of Prx1-GFP$^+$ cells as were PαS cells (11.6±5.3%), as shown in Fig. 3A, we used only Sca1 antibody to distinguish cells with MSCs properties among Prx1-GFP$^+$ cells. Prx1-GFP$^+$Sca1$^+$ populations highly expressed CD51, CD61 and CD90, in addition to PDGFRα (97.7±1.9%), indicating that almost all Prx1-GFP$^+$Sca1$^+$ cells should be Prx1-GFP$^+$PαS cells with MSC properties. By contrast, Prx1-GFP$^+$Sca1$^-$ populations displayed lower expression levels of CD61, CD90, CD105 and PDGFRα (36.7±11.1%) (Fig. 3B; Fig. S11B). These results clearly show that calvarial Prx1$^+$Sca1$^+$ cells are a more homogeneous population than Prx1$^+$Sca1$^-$ cells in terms of the expression profiles of conventional MSC surface markers.

We next determined Runx2 expression levels as well as the self-renewal and multi-lineage differentiation potential of Prx1$^+$Sca1$^+$ and Prx1$^+$Sca1$^-$ cells. A colony-forming unit-fibroblast assay revealed that the colony-forming capacity of Prx1-GFP$^+$Sca1$^+$ cells was greater than that of Prx1-GFP$^+$Sca1$^-$ cells (5.8% versus 0.14%, respectively; Fig. 3C). Furthermore, Prx1-GFP$^+$Sca1$^+$ cells robustly differentiated into osteoblasts and adipocytes, whereas Prx1-GFP$^+$Sca1$^-$ cells

Development (2016) 143, 211-218 doi:10.1242/dev.128793

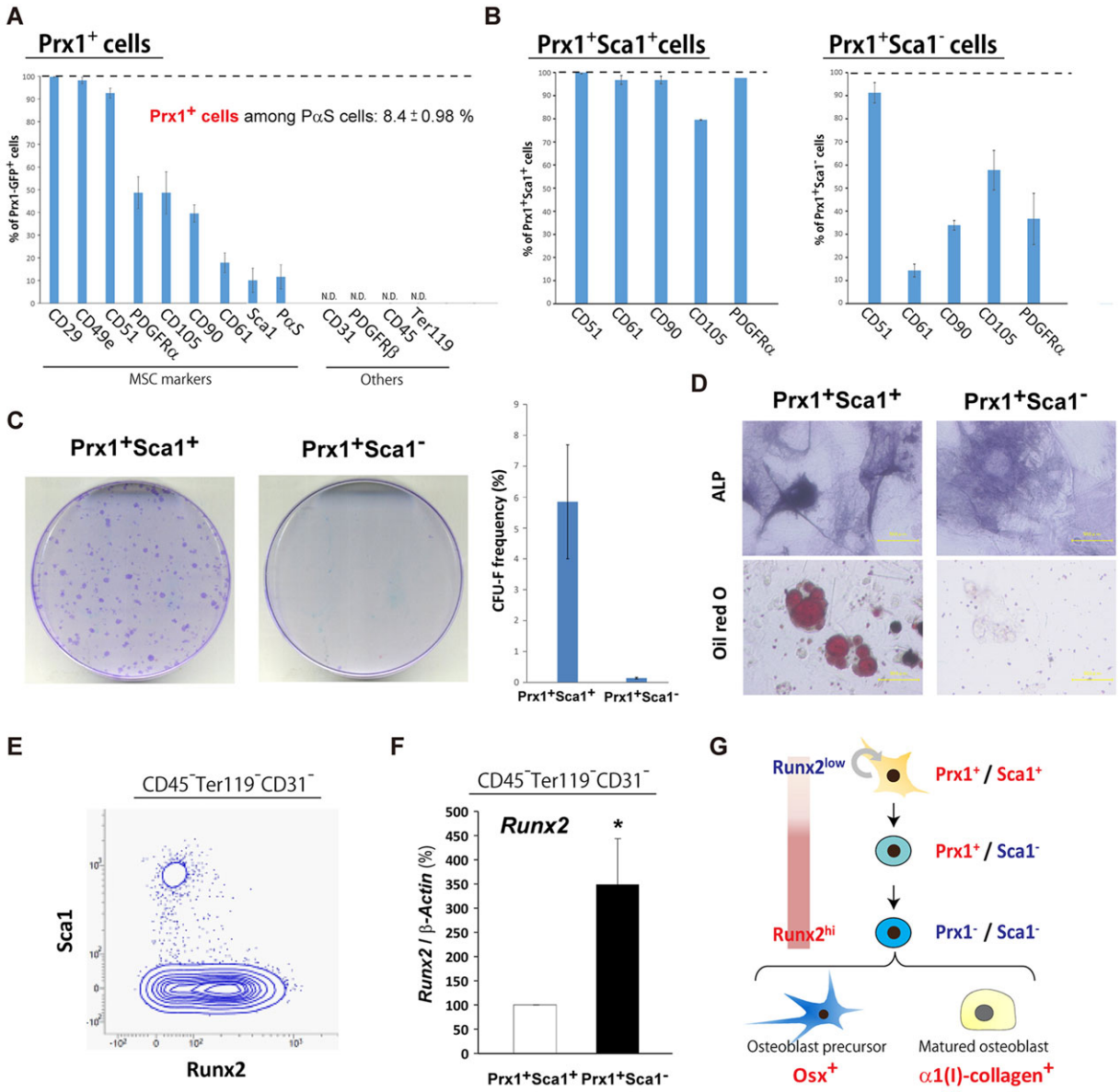

Fig. 3. Prx1^{+}Sca1^{+} cells have multipotent and self-renewal potential with lower Runx2 expression. (A) Prx1-GFP^{+} cells were analyzed for the expression of the indicated cell surface markers by flow cytometry (n=4-6). N.D., not detected. (B) Calvarial Prx1^{+}Sca1^{+} or Prx1^{+}Sca1^{-} cells were analyzed for cell surface markers by flow cytometry (n=3). Error bars indicate s.e.m. (C) Frequency of colony-forming unit-fibroblasts (CFU-Fs) detected at 10 days after plating Prx1^{+}Sca1^{+} and Prx1^{+}Sca1^{-} cells (n=5). (D) Differentiation of a colony of Prx1^{+}Sca1^{+} and Prx1^{+}Sca1^{-} cells into osteoblasts and adipocytes, respectively. Scale bars: 50 µm. (E) Stromal (CD45^{-}Ter119^{-}CD31^{-}) calvarial cells were analyzed for the expressions of Runx2 and Sca1 by flow cytometry. (F) Stromal Prx1^{+}Sca1^{+} or Prx1^{+}Sca1^{-} cells were sorted from the calvaria of *Prx1-GFP* mice at P1, followed by determination of *Runx2* mRNA expression by qPCR (n=4). *P<0.05; Student's t-test. Error bars indicate s.e.m. (G) Schematic of the cell fate of Prx1^{+}Sca1^{+} cells in the calvaria. Stepwise differentiation of Prx1^{+}Sca1^{+} cells into Prx1^{-}Sca1^{-} cells, which include osterix^{+} osteoblast precursor and α1(I)-collagen^{+} matured osteoblasts.

differentiated into osteoblasts, but not adipocytes (Fig. 3D). Among total calvarial stromal cells, Sca1 expression was clearly inversely proportional to Runx2 expression (Fig. 3E). Moreover, immunohistochemical analyses revealed that Sca1 expression was observed in periosteum and intrasutural mesenchyme (Fig. S12A,B). Prx1-GFP^{+}Sca1^{+} cells were observed in a small part of intrasutural mesenchyme and expressed Runx2 at a lower level compared with that in Prx1-GFP^{+}Sca1^{-} cells (Fig. S12C). In addition, mRNA expression of *Runx2* and MSC markers (*Itgb3* and *Thy1*) was significantly higher (*Runx2*) and lower (*Itgb3* and *Thy1*) in Prx1-GFP^{+}Sca1^{-} cells than in Prx1-GFP^{+}Sca1^{+} cells (Fig. 3F; Fig. S13), supporting the notion of heterogeneous Runx2 expression in Prx1-GFP^{+} cells as indicated by the data shown in Fig. S7.

These results suggest that multipotent self-renewing cells were present in the Prx1^{+}Sca1^{+} subsets with lower Runx2 expression, rather than in the Prx1^{+}Sca1^{-} cells with higher Runx2 expression, in the calvaria (Fig. 3G).

Runx2 is also required for intramembranous ossification through its expression in osterix (Osx)$^{+}$ osteoblast precursors

Osx is another transcriptional determinant of osteoblast lineages expressed by osteoblast precursors downstream of Runx2 (Nakashima et al., 2002). Osx^{+} osteoblast precursors differentiate further into mature osteoblasts that produce α1(I)-collagen (Maes et al., 2010). *Runx2*$_{prx1}^{-/-}$ mice were deficient in intramembranous

Development (2016) 143, 211-218 doi:10.1242/dev.128793

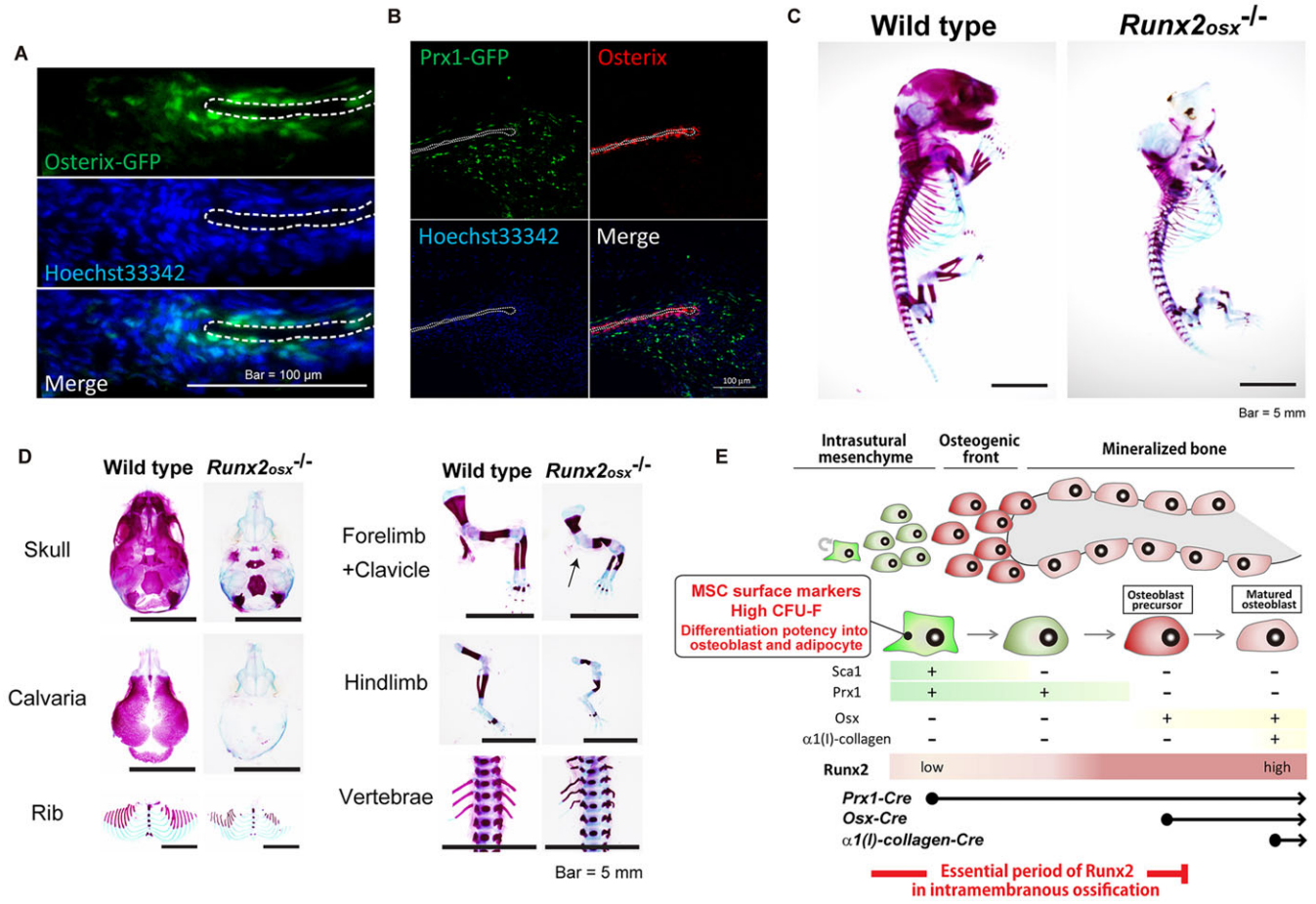

Fig. 4. Runx2 in Osx^{+} cells regulates skeletogenesis. (A) Confocal image of the sagittal suture of Osx-GFP^{+} mice at P1. Dashed line indicates the border of mineralized bone. (B) Confocal image of the sagittal suture of *Prx1-GFP* mice at P1. The sections were stained with an anti-Osx antibody (red). Scale bars: 100 µm. (C) Skeletons of wild-type (WT) and *Runx2*$_{osx}^{-/-}$ mice at E18.5. Embryos were double stained with Alizarin Red and Alcian Blue. Scale bars: 5 mm. (D) Parts of skeletons from WT and *Runx2*$_{osx}^{-/-}$ mice at E18.5. The clavicle was absent in *Runx2*$_{osx}^{-/-}$ mice (arrow). Scale bars: 5 mm. (E) Schematic summarizing the findings of this study. Multipotent self-renewing Prx1^{+}Sca1^{+} cells differentiate into α1(I)-collagen^{+} osteoblasts stepwise in calvaria. Runx2 has an essential function in intramembranous ossification until the Osx^{+}Prx1^{-}Sca1^{-} osteoblast precursor stage during the differentiation steps of Prx1^{+}Sca1^{+} cells.

ossification in parietal bone, whereas *Runx2*$_{col(I)}^{-/-}$ mice showed no skeletal abnormalities. In addition, as shown in Fig. 2B and Fig. S6A, Runx2 was strongly expressed in Prx1-GFP^{-} cells at the osteogenic front and the bony plate surface in the calvaria. Moreover, *Runx2* mRNA expression was markedly higher in calvarial osteoblasts compared with that in Prx1-GFP^{+} cells (Fig. S9A). We therefore investigated whether Runx2 in cells of the Osx lineage played a role in intramembranous ossification. In parietal bone of *Osx-Cre* transgenic mice expressing the GFP::Cre fusion protein, almost all Osx-GFP^{+} cells were positioned at the osteogenic front and the surface of mineralized bone (Fig. 4A), in which Prx1-GFP^{+} cells are absent and Runx2 is highly expressed (Fig. 2B; Fig. S7). Moreover, immunohistochemical analyses revealed that Osx was highly expressed in Prx1-GFP^{-} cells at the bony plate surface (mineralized bone) (Fig. 4B), suggesting that Osx is highly expressed by Prx1^{-}Runx2^{+} cells in parietal bone. Although *Osx-Cre;Runx2*$^{flox/flox}$ (*Runx2*$_{osx}^{-/-}$) embryos were alive at E18.5, *Runx2*$_{osx}^{-/-}$ mice died at birth, similar to *Runx2*$^{-/-}$ mice, *Runx2*$_{col(II)}^{-/-}$ mice (Takarada et al., 2013) and *Runx2*$_{prx1}^{-/-}$ mice. Skeletal analysis of E18.5 *Runx2*$_{osx}^{-/-}$ mice revealed severe mineralization defects in the calvaria, scapula, humerus, radius, ulna, femur, tibia, fibula, sternum and clavicle (Fig. 4C,D). These results clearly revealed that Runx2 is essential for intramembranous ossification through its expression in cells of the Osx lineage.

Our results suggest that osteoblast differentiation in the calvaria begins at the Prx1^{+}Sca1^{+} MSC stage with sequential progression to Prx1^{+}Sca1^{-} cells, then Osx^{+}Prx1^{-}Sca1^{-} osteoblast precursors, which eventually form mature α1(I)-collagen^{+} osteoblasts. Furthermore, during the stepwise differentiation of Prx1^{+}Sca1^{+} MSCs into mature α1(I)-collagen^{+} osteoblasts, the essential period of Runx2 function in intramembranous ossification probably begins at the Prx1^{+}Sca1^{+} MSC stage and ends at the Osx^{+}Prx1^{-}Sca1^{-} osteoblast precursor stage [before the mature α1(I)-collagen^{+} osteoblasts appear] (Fig. 4E). Although intensive studies have been conducted to identify the functional importance of Runx2 in osteoblast differentiation, to the best of our knowledge, this is the first report showing direct evidence of the cellular origin and essential period of Runx2 function during intramembranous ossification.

MATERIALS AND METHODS

Experimental animals and skeletal preparation

Prx1-Cre, *Nestin-Cre*, *Osx-Cre* and Rosa26-tdTomato mice were from Jackson laboratory [B6.Cg-Tg(Prrx1-cre)1Cjt/J, B6.Cg-Tg(Nes-cre)

Development (2016) 143, 211-218 doi:10.1242/dev.128793

1Kln/J, B6.Cg-Tg(Sp7-tTA,tetO-EGFP/cre)1Amc/J and B6.Cg-Gt(ROSA)26Sortm14(CAG-tdTomato)Hze/J, respectively]. *Runx2* conditional knockout mice lacking exon 4 of the *Runx2* gene (*Runx2*$^{flox/+}$) were bred in our animal facility. *Prx1-GFP* mice, *Nestin-GFP* mice and *α1(I)-collagen-Cre* mice were provided by Dr Murakami (Case Western Reserve University, OH, USA), Dr Enikolopov (Cold Spring Harbor Laboratory, NY, USA) and Dr Karsenty (Columbia University, NY, USA), respectively. The protocol employed here meets the guideline of the Japanese Society for Pharmacology and was approved by the Committee for Ethical Use of Experimental Animals at Kanazawa University. The numbers of samples and sections used per experiment are stated in the figure legends.

Skeletal double staining with Alcian Blue and Alizarin Red was performed as described previously (Takahata et al., 2012). Sections were stained with Hematoxylin and Eosin (H&E), von Kossa and Alcian Blue stains.

Immunofluorescence staining

Neonatal mouse calvaria were fixed with 4% paraformaldehyde, followed by immersion in 30% sucrose. Calvaria were then embedded in OCT and cryosectioned at 14 µm (Leica CM 3050), followed by immunostaining with specific antibodies (Table S1). Confocal images were acquired using LSM710 and Zen2009 software (Zeiss).

Flow cytometry and cell sorting

Neonatal parietal and frontal calvaria (including coronal and sagittal suture) were dissected and washed several times in PBS, followed by treatment with 125 mM EDTA for 10 min (twice) for decalcification. Decalcified calvaria were next treated with 0.2% collagenase (Wako) in PBS at 37°C for 20 min. No cells were collected from calvaria by further collagenase digestion. Calvarial cells were collected by centrifugation (160 ***g***), followed by soaking in water for 5 to 10 s in order to burst the blood cells. Finally, cells were suspended in 2% fetal bovine serum (FBS) in PBS for the staining with fluorescence-labeled antibodies (Table S1). Flow cytometric analysis was carried out using the FACS Verse (BD Biosciences). Data were analyzed by FACS Suite software (BD Biosciences). Cell sorting experiments were performed using an Aria Cell sorter (BD Biosciences).

Colony-forming unit-fibroblast (CFU-F) assay and *in vitro* differentiation

For the CFU-F assay, 1500 or 3000 sorted cells were plated in 90-mm dishes (Nunc) in DMEM (Wako) supplemented with 20% FBS (HyClone), and incubated for 10 days at 37°C under 5% CO_2. CFU-F colonies were counted after Crystal Violet staining. Osteoblastic differentiation was induced by osteogenic inducer (L-ascorbic acid and β-glycerophosphate), and subsequent alkaline phosphatase staining. Adipogenic differentiation was performed using adipogenic inducers (dexamethasone, pioglitazone, insulin and 3-isobutyl-1-methylxanthine) for the first 2 days, followed by culture with pioglitazone and insulin for a further 14 days, and subsequent Oil Red O staining.

RNA isolation and quantitative RT-PCR (qPCR) analysis

Sorted cells were lysed in Buffer RLT (QIAGEN), and RNA isolation was performed using the RNeasy Mini Kit (QIAGEN). Quantitative real-time PCR was performed using specific primers. The sequences used as primers were as follows: *Runx2*, 5′-CCTAGTTAGAGTGGTAGCAGAAG-C-3′, 5′-ACAGACAACGAAGAAAGTTCCCAC-3′; *Itgb3*, 5′-CCACACG-AGGCGTGAACTC-3′, 5′-CTTCAGGTTACATCGGGGTGA-3′; *Thy1*, 5′-CCAACCAGCCCTATATCAAGGT-3′, 5′-TGAAGCTCACAAAAGT-AGTCGC-3′; *Actb*, 5′-GGCTCCTAGCACCATGAAGATCAAG-3′, 5′-A-TCTGCTGGAAGGTGGACAGTGAG-3′. The relative mRNA expression was determined using the ΔCt method. The gene expression was normalized to *Actb*.

Culture of osteoblasts and Alizarin Red/Van Gieson staining

Primary osteoblasts were prepared from the mouse calvariae at E18.5 by the sequential enzymatic digestion method, as previously described (Takarada et al., 2013). A differentiation-inducing mixture containing 50 µg/ml ascorbic acid and 5 mM β-glycerophosphate was used for the culture of primary osteoblasts. For Alizarin Red and Van Gieson staining, cultured cells were stained with Alizarin Red S (Sigma) or Weigert's iron Hematoxylin (Sigma)/Van Gieson's solution (Wako), respectively.

Statistical analysis

Quantitative data are expressed as mean±s.e.m. Statistical significance of differences was determined using Student's *t*-test (Fig. 3F; Fig. S1B; Fig. S4B; Fig. S9A; Fig. S13). Differences were considered significant at $P<0.05$.

Acknowledgements

We are very grateful to Drs S. Murakami (Case Western Reserve University, OH, USA) and G. Enikolopov (Cold Spring Harbor Laboratory, NY, USA) for generously providing *Prx1-GFP* mice and *Nestin-GFP* mice, respectively. We also thank Dr Gerard Karsenty for critical reading of the manuscript.

Competing interests

The authors declare no competing or financial interests.

Author contributions

T.T. and E.H. developed the concept of the study. T.T., R.N., A.T., K.F., T.I., Y.Y. and E.H. performed experiments. T.T. and R.N. analyzed data. T.T. and E.H. wrote the manuscript.

Funding

This work was supported in part by Grants-in-Aid for Scientific Research [26460387 to T.T. and 23689004 to E.H.] from the Ministry of Education, Culture, Sports, Science and Technology, Japan; and in part by research grants to T.T. from the Takeda Science Foundation, the Kanzawa Medical Research Foundation, the ONO Medical Research Foundation, the Uehara Memorial Foundation and the NOVARTIS Foundation (Japan) for the Promotion of Science.

Supplementary information

Supplementary information available online at
http://dev.biologists.org/lookup/suppl/doi:10.1242/dev.128793/-/DC1

References

Chai, Y. and Maxson, R. E., Jr. (2006). Recent advances in craniofacial morphogenesis. *Dev. Dyn.* **235**, 2353-2375.

Cserjesi, P., Lilly, B., Bryson, L., Wang, Y., Sassoon, D. A. and Olson, E. N. (1992). MHox: a mesodermally restricted homeodomain protein that binds an essential site in the muscle creatine kinase enhancer. *Development* **115**, 1087-1101.

Ducy, P., Zhang, R., Geoffroy, V., Ridall, A. L. and Karsenty, G. (1997). Osf2/Cbfa1: a transcriptional activator of osteoblast differentiation. *Cell* **89**, 747-754.

Hall, B. K. and Miyake, T. (1992). The membranous skeleton: the role of cell condensations in vertebrate skeletogenesis. *Anat. Embryol.* **186**, 107-124.

Jiang, X., Iseki, S., Maxson, R. E., Sucov, H. M. and Morriss-Kay, G. M. (2002). Tissue origins and interactions in the mammalian skull vault. *Dev. Biol.* **241**, 106-116.

Kawanami, A., Matsushita, T., Chan, Y. Y. and Murakami, S. (2009). Mice expressing GFP and CreER in osteochondro progenitor cells in the periosteum. *Biochem. Biophys. Res. Commun.* **386**, 477-482.

Komori, T., Yagi, H., Nomura, S., Yamaguchi, A., Sasaki, K., Deguchi, K., Shimizu, Y., Bronson, R. T., Gao, Y.-H., Inada, M. et al. (1997). Targeted disruption of Cbfa1 results in a complete lack of bone formation owing to maturational arrest of osteoblasts. *Cell* **89**, 755-764.

Kronenberg, H. M. (2003). Developmental regulation of the growth plate. *Nature* **423**, 332-336.

Lendahl, U., Zimmerman, L. B. and McKay, R. D. G. (1990). CNS stem cells express a new class of intermediate filament protein. *Cell* **60**, 585-595.

Logan, M., Martin, J. F., Nagy, A., Lobe, C., Olson, E. N. and Tabin, C. J. (2002). Expression of Cre Recombinase in the developing mouse limb bud driven by a Prxl enhancer. *Genesis* **33**, 77-80.

Maes, C., Kobayashi, T., Selig, M. K., Torrekens, S., Roth, S. I., Mackem, S., Carmeliet, G. and Kronenberg, H. M. (2010). Osteoblast precursors, but not mature osteoblasts, move into developing and fractured bones along with invading blood vessels. *Dev. Cell* **19**, 329-344.

Méndez-Ferrer, S., Michurina, T. V., Ferraro, F., Mazloom, A. R., MacArthur, B. D., Lira, S. A., Scadden, D. T., Ma'ayan, A., Enikolopov, G. N. and Frenette, P. S. (2010). Mesenchymal and haematopoietic stem cells form a unique bone marrow niche. *Nature* **466**, 829-834.

Development (2016) 143, 211-218 doi:10.1242/dev.128793

Mignone, J. L., Kukekov, V., Chiang, A.-S., Steindler, D. and Enikolopov, G. (2004). Neural stem and progenitor cells in nestin-GFP transgenic mice. *J. Comp. Neurol.* **469**, 311-324.

Morikawa, S., Mabuchi, Y., Kubota, Y., Nagai, Y., Niibe, K., Hiratsu, E., Suzuki, S., Miyauchi-Hara, C., Nagoshi, N., Sunabori, T. et al. (2009). Prospective identification, isolation, and systemic transplantation of multipotent mesenchymal stem cells in murine bone marrow. *J. Exp. Med.* **206**, 2483-2496.

Mundlos, S., Otto, F., Mundlos, C., Mulliken, J. B., Aylsworth, A. S., Albright, S., Lindhout, D., Cole, W. G., Henn, W., Knoll, J. H. M. et al. (1997). Mutations involving the transcription factor CBFA1 cause cleidocranial dysplasia. *Cell* **89**, 773-779.

Nakashima, K., Zhou, X., Kunkel, G., Zhang, Z., Deng, J. M., Behringer, R. R. and de Crombrugghe, B. (2002). The novel zinc finger-containing transcription factor osterix is required for osteoblast differentiation and bone formation. *Cell* **108**, 17-29.

Ono, N., Ono, W., Mizoguchi, T., Nagasawa, T., Frenette, P. S. and Kronenberg, H. M. (2014). Vasculature-associated cells expressing nestin in developing bones encompass early cells in the osteoblast and endothelial lineage. *Dev. Cell* **29**, 330-339.

Otto, F., Thornell, A. P., Crompton, T., Denzel, A., Gilmour, K. C., Rosewell, I. R., Stamp, G. W. H., Beddington, R. S. P., Mundlos, S., Olsen, B. R. et al. (1997). Cbfa1, a candidate gene for cleidocranial dysplasia syndrome, is essential for osteoblast differentiation and bone development. *Cell* **89**, 765-771.

Takahata, Y., Hinoi, E., Takarada, T., Nakamura, Y., Ogawa, S. and Yoneda, Y. (2012). Positive regulation by gamma-aminobutyric acid B receptor subunit-1 of chondrogenesis through acceleration of nuclear translocation of activating transcription factor-4. *J. Biol. Chem.* **287**, 33293-33303.

Takarada, T., Hinoi, E., Nakazato, R., Ochi, H., Xu, C., Tsuchikane, A., Takeda, S., Karsenty, G., Abe, T., Kiyonari, H. et al. (2013). An analysis of skeletal development in osteoblast-specific and chondrocyte-specific runt-related transcription factor-2 (Runx2) knockout mice. *J. Bone Miner. Res.* **28**, 2064-2069.

Yoshida, T., Vivatbutsiri, P., Morriss-Kay, G., Saga, Y. and Iseki, S. (2008). Cell lineage in mammalian craniofacial mesenchyme. *Mech. Dev.* **125**, 797-808.

Zimmerman, L., Lendahl, U., Cunningham, M., McKay, R., Parr, B., Gavin, B., Mann, J., Vassileva, G. and McMahon, A. (1994). Independent regulatory elements in the nestin gene direct transgene expression to neural stem cells or muscle precursors. *Neuron* **12**, 11-24.